

Review Article

Open Access

Properties of $\text{ZnS}_{1-x}\text{Fe}_x$ thin Films Deposited

Jafarli Rufat

Baku State University, Azerbaijan

ABSTRACT

Semiconducting $\text{ZnS}_{1-x}\text{Fe}_x$ thin films were prepared with different substrate temperature on glass substrates from aqueous solution technique. $\text{ZnS}_{1-x}\text{Fe}_x$ films were prepared, using a aqueous solution containing ethyleneglycol, zinc chloride and sulphur. XRD study shows that the aqueous deposited $\text{ZnS}_{1-x}\text{Fe}_x$ thin films are polycrystalline hexagonal structure. The effect of Fe concentration on the optical parameters such as absorption coefficient, refractive index, dielectric function, optical conductivity, and reflectivity is also investigated. Results revealed that $\text{Cd}_{1-x}\text{Fe}_x\text{S}$ is a suitable compound for spintronics and optoelectronics devices. A good optical transparency of about 75% in the visible region is observed for all prepared $\text{ZnS}_{1-x}\text{Fe}_x$ thin films. The direct optical band gap of the deposited $\text{ZnS}_{1-x}\text{Fe}_x$ thin films with different substrate temperature (380°C – 530°C) were lying in the range 3.27–3.35 eV.

*Corresponding author

Jafarli Rufat, Baku State University, Azerbaijan. Ph: +994552961310; E-mail: r.c_89@mail.ru

Received: November 07, 2021; Accepted: November 11, 2021; Published: November 16, 2021

Keywords: Fe-doped ZnS, First Principles Calculation, Ferromagnetic Properties

Introduction

Binary semi-conducting thin films of the type II – VI have received considerable attention for their optical, electrical and photo induced properties [1-3]. This class of thin films has been extensively studied recently, partly as an interesting subject for fundamental research and partly due to potential applications in optoelectronic devices, solar cells, IR detectors and lasers. Semi-conducting ZnS thin films have a high refractive index of 2.27 at 1 μm , high transmittance in the visible range, and large direct band gap of 3.6 eV in near UV region. ZnS is an excellent optical material in the infrared and far-infrared region [4-6]. Thin films of ZnS were prepared using many deposition techniques such as chemical bath deposition CBD, in this paper $\text{ZnS}_{1-x}\text{Fe}_x$ chalcogenide thin films have been deposited on glass substrate from a aqueous solution with different substrate temperature using chemical bath deposition [7]. ZnSFe films were prepared using a aqueous solution containing ethylene glycol, zinc chloride, and sulphur. The properties of the prepared thin films were obtained using the XRD and optical absorption techniques.

Experimental

Zinc sulfide thin films were prepared on glass substrates (area 1.5 x 4.0 cm^2) using pyrolysis technique. The glass substrates were cleaned by soapy water in an ultrasonic bath, and rinsed thoroughly in deionized water and alcohol respectively. Aqueous ethylene glycol solution containing zinc chloride, iron chloride and thiocarbamide were used to prepare $\text{ZnS}_{1-x}\text{Fe}_x$ deposited thin films. Un-doped and iron doped ZnS thin films were deposited on glass substrates by the CBD method at acidic value of pH (4.5). Appropriate quantities of zinc chloride, iron chloride, thioacetamide and urea were weighed according to the stoichiometry and were dissolved in deionized water to make 0.15, 0.15, 1 and 5 M solutions respectively. The aqueous solutions of thiocarbamide and urea were added drop wise to

the solution of zinc chloride under vigorous stirring at room temperature. Hydrochloric acid (0.5 M) was used to control the pH of solution. After complete dissolution of thioacetamide and urea in zinc chloride, a transparent solution was obtained. At this stage, suitable volumes of iron chloride solution depending on the desired doping concentration were added drop wise to the solution containing zinc chloride and thioacetamide. It is worth mentioning that the whole synthesis was performed without use of any surfactant or capping agent. After complete dissolution of iron chloride, the final solution was transferred to chemical bath and maintained at 90°C under magnetic stirring. The lower part of the reaction chamber heated by electrical resistance and substrate temperature was measured with a thermocouple. The substrate temperature has varied between 350–500°C. Thickness of prepared thin films was obtained by a micro gravimetric method. The films were deposited on glass substrates whose mass was previously determined. After the deposition, the substrates were again weighed, determining the quantity of deposited $\text{ZnS}_{1-x}\text{Fe}_x$.

The thickness for all prepared thin films is about 260 nm. The structural properties of the $\text{ZnS}_{1-x}\text{Fe}_x$ thin films were studied by a Philips PW 1710 X-ray diffractometer using $\text{CuK}\alpha$ radiation of wavelength $\lambda = 1.5405 \text{ \AA}$ in the range of 2θ between 10° and 60°. The optical transmission spectra of the deposited thin films were measured in the wavelength region $\lambda = 300 - 1100 \text{ nm}$ by a UV spectrophotometer Shimadzu – 3101.

Results and Discussion

XRD peaks of spray deposited zinc sulfide thin films prepared out of aqueous solution onto a glass substrate are shown in Figure (1). The XRD patterns (Fig. 1) show the poly and nanocrystalline nature of Fe doped ZnS thin films. The observed diffraction peaks correspond to (111), (220) and (311) lattice planes and are well matched with the standard pattern of cubic zinc blende ZnS (ICCD # 01-005-0566). The effect of Fe incorporation in ZnS is evident from shift of diffraction peak corresponding to (111) plane from standard 2θ of 28.861 to the smaller 2θ values, since the ionic

radii of iron is slightly bigger than that of zinc. The change in lattice constant of ZnS resulted from iron incorporation was also observed. The XRD results reveal that the crystallinity of ZnS thin films decreases as the dopant's concentration increases. The average crystallite size was estimated by Scherrer's formula as $D \propto \frac{k\lambda}{\beta \cos \theta}$ where D is the average crystallite size, k is the geometric factor, λ is the X-ray wavelength of Cu $K\alpha$ radiations (1.5405 Å), β is the full width at half-maximum of diffraction peaks, and θ is the Bragg diffraction angle. Crystallite sizes calculated by Scherrer's equation for Fe doped ZnS thin films are listed in Table 1. Fig. 2 shows the variation of lattice constant and crystallite size as a function of dopant's concentration. The crystallite size variation also supports the evidence of reduction in crystallinity of thin films with increased iron doping. The reduction in crystallite size with the increase of iron content in the ZnS crystals has been reported earlier and confirmed by band gap calculations.

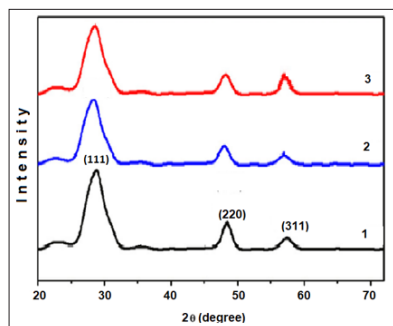


Figure 1: XRD patterns of Fe doped ZnS thin films with 0.5 (1), 2.0 (2), and 5.0 (3) at% of iron, respectively.

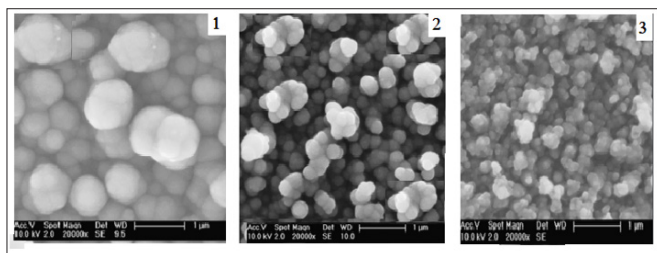


Figure 2: SEM images of Fe doped ZnS thin films with 0.5 (1), 2.0 (2), and 5.0 (3) at% of iron, respectively

The transmittance of the thin films deposited on glass substrates measured in the wavelength region 300-1100 nm by subtracting the transmittance of the glass substrate taken as a reference. A good optical transparency of about 75% in the visible region is observed for all $\text{ZnS}_{1-x}\text{Fe}_x$ thin films. Figure 3 shows some rise and fall in the transmittance spectra of thin film deposited with substrate temperature 420°C which disappears in spectra of thin film deposited with substrate temperature 380°C. Such rise and fall are attributed to the interference of light transmitted through the thin films. Below 400 nm there is a sharp fall in the transmittance of the films, which is due to the strong absorbance of the films in this region.

The higher transmittance for a higher deposition annealing temperature and the sharp increase of transmittance at the band edge are attributed to the good crystallinity owing to small concentration of structural defects. Extinction coefficient k versus wavelength λ spectra is shown in Figure 2. In the visible range, extinction coefficient is approximately constant and decreases with increasing substrate temperature. The increased extinction

coefficient at the wavelengths below 400 nm is due to the high absorbance of $\text{ZnS}_{1-x}\text{Fe}_x$ thin films in that region.

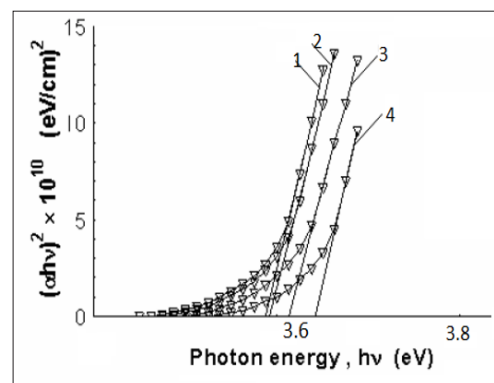


Figure 3: Plot to determine the direct bandgap of $\text{ZnS}_{1-x}\text{Fe}_x$ deposited thin films from aqueous solution with different annealing temperatures.

Absorption coefficient α can be used to determine the band gap of the material. The values of the band gap for the direct transition can be determined by extrapolating the straight line portion of the $(\alpha h\nu)^2$ versus $h\nu$ graphs to the $h\nu$ axis. $(\alpha h\nu)^2$ versus $h\nu$ plots for $\text{ZnS}_{1-x}\text{Fe}_x$ thin films annealing with different temperatures are shown in Figure 3. Direct band gap energy of $\text{Zn}_{1-x}\text{Fe}_x\text{S}$ thin films increases from 3.38 eV to 3.46 eV as deposition substrate temperature increases from 380 to 530°C at film thickness 260 nm.

The temperature-dependent magnetization (M - T) curve for single-phase Fe-doped ZnS sample are measured using a SQUID magnetometer with a magnetic field of 1000Oe, applied perpendicular to the film plane. Measurements are taken at the relatively large applied magnetic field in order to increase the magnetic signal from thin film with respect to the large diamagnetic response of the Si substrate. Measurements have also been taken at 3000Oe and shown similar temperature dependence. The results of magnetization subtract of the diamagnetic contribution of the Si substrate. The dc zero-field-cooled (ZFC) and the field-cooled (FC) magnetization curves are shown in Fig 4. Measurements are performed from 5 to 300K. The FC is obtained by measuring the magnetic moment of the sample in a magnetic field of 1000 Oe during cooling. The ZFC measurement is obtained by first cooling the sample to 5 K in zero fields and then warming it in the same field as that of the FC measurement. The ZFC magnetization shows stronger temperature dependence than the FC one below 30 K. ZFC and the FC magnetization curves are measured overlap after high temperature about 180K with a paramagnetic behavior. Fig.3 displays a ferromagnetic behavior persisting up to 270K.

Figure 5 displays the results of magnetization as a function of applied magnetic field measured for ZnS:Fe film at 100K. The total magnetization could be described as an algebraic sum of various contributions. The substrate diamagnetic contribution is subtracted from the total magnetization signal. The remaining data consist of the paramagnetic and ferromagnetic contributions from the ZnS:Fe thin film. The well-defined hysteresis loops show that the ZnS:Fe film are clearly ferromagnetic at 100 K. At 100 K, the saturation magnetization (M_S) is 1.82×10^{-5} emu with a remanence magnetization (M_R) of 0.31×10^{-5} emu and a coercive field (H_C) of 50 Oe. Si substrate and ZnS are diamagnetic, so the magnetization data indicate that the ferromagnetization in the present study is because Fe-doped in ZnS thin film and formed ZnS:Fe DMS.

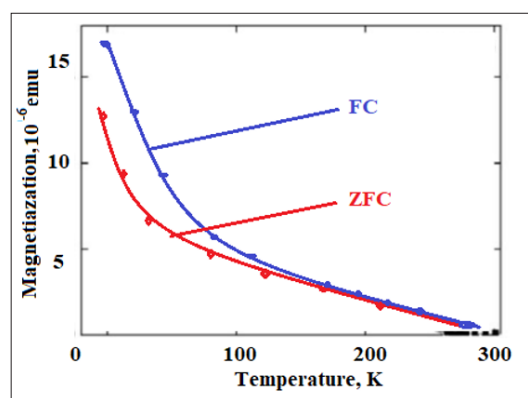


Figure 4: The FC-ZFC M-T curve of the Fe-doped ZnS shows temperature-dependent magnetization of both zero – field – cooled (down – curve) and field – cooled (up-curve) in the field of 1.0 KOe.

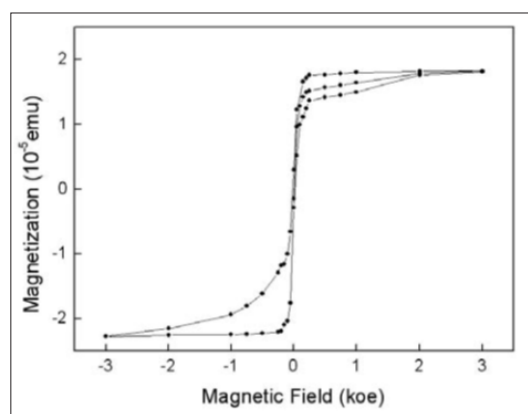


Figure 5: M-H curve of the sample taken at 100 K after the necessary background diamagnetic subtraction, the magnetic field used is from 0 up to 0.3 T.

The origin of the ferromagnetism in DMS materials is still not clearly understood. To further demonstrate that the Fe-doped ZnS thin films are favorable for high temperature ferromagnetism, we model 64-atom cell to simulate the magnetic interactions of Fe atoms by performing first principles spin-polarized density functional theory (DFT) calculations within generalized-gradient approximation (GGA). We can find that these magnetic interactions are mainly strong p-d coupling between the Fe 3d states and S 2p states. The calculated total energy differences between ferromagnetic (FM) and anti-ferromagnetic (AFM) configuration ($\Delta E = E_{FM} - E_{AFM}$) are 46 meV, indicating that ferromagnetic ordering is favorable for ZnS:Fe system. Therefore, the observed ferromagnetism should be the intrinsic behavior of Fe-doped ZnS thin film.

Conclusions

Zinc sulfide thin films have been deposited and annealing with different temperature from aqueous solution containing ethylene glycol, zinc chloride, SeO and sulphur. XRD study shows that the deposited $\text{ZnS}_{1-x}\text{Se}_x$ thin films onto glass substrates are polycrystalline hexagonal structure. Prepared $\text{ZnS}_{1-x}\text{Se}_x$ thin films have a good optical transparency of about 75 % in the visible region. Extinction coefficient, refractive index, dielectric constant, and optical conductivity were calculated from optical reflectance and optical absorption values. The direct band gap of the $\text{ZnS}_{1-x}\text{Se}_x$ thin films increases as the deposition substrate temperature increases. In summary, we have reported the ferromagnetic properties of

single-phase ZnS:Fe thin films prepared on Si substrates by CBD as a new method. Field and temperature dependent magnetization curve indicated that a high curie temperature $T_c = 270\text{K}$.

References

1. S Mirov, V Fedorov, I Moskalev, M Mirov, D Martyshkin et al. (2013) Mid-IR lasers based on transition metal and rare-earth ion doped crystals 133: 268.
2. M Gloeckler, I Sankin, Z Zhao (2013) CdTe Solar Cells at the Threshold to 20% Efficiency IEEE J Photovolt 3: 1389.
3. PM Farias, BS Santos, AA de Thomaz, R Ferreira, FD Menezes et al (2008) J Phys. Chem B 112: 2734.
4. Arvind P Ravikumar, Thor A Garcia, Joel De Jesus, Maria C Tamargo, Claire F Gmachl (2015) Long wave, room temperature II-VI-based quantum cascade emitters Appl Phys Lett 107: 141105.
5. J Li, DR Diercks, TR Ohno, CW Warren, MC Lonergan, et al. (2015) Sol Energy Mater Sol Cells 133: 208.
6. TA Gessert, S Asher, S Johnston, M Young, P Dipppo, C Corwine (2017) Thin Solid Films 515: 6103.
7. DU Lee, SP Kim, KS Lee, SW Pak, EK Kim (2013) Appl Phys Lett 103: 263901.
8. T Nakasu, M Kobayashi, H Togo, T Asahi (2014) Growth and characterization of ZnTe layers on severely lattice mismatched sapphire substrates by MBE J Electron Mater 43: 921.

Copyright: ©2021 Jafarli Rufat. This is an open-access article distributed under the terms of the Creative Commons Attribution License, which permits unrestricted use, distribution, and reproduction in any medium, provided the original author and source are credited.